European Journal of Medicinal Chemistry 101 (2015) 266–273

Contents lists available at ScienceDirect

European Journal of Medicinal Chemistry

journal homepage: http://www.elsevier.com/locate/ejmech

Research paper

Primaquine–pyrimidine hybrids: Synthesis and dual-stage antiplasmodial activity

Hardeep Kaur [a], Marta Machado [d], Carmen de Kock [b], Peter Smith [b], Kelly Chibale [c], Miguel Prudêncio [d], Kamaljit Singh [a, *]

[a] Department of Chemistry, UGC-Centre for Advanced Studies-II, Guru Nanak Dev University, Amritsar 143005, India
[b] Division of Pharmacology, Department of Medicine, University of Cape Town, Observatory 7925, South Africa
[c] Department of Chemistry, South African Medical Research Council Drug Discovery and Development Research Unit, Institute of Infectious Disease and Molecular Medicine, University of Cape Town, Rondebosch 701, South Africa
[d] Instituto de Medicina Molecular, Faculdade de Medicina da Universidade de Lisboa, Av. Prof. Egas Moniz, 1649-028 Lisboa, Portugal

ARTICLE INFO

Article history:
Received 21 March 2015
Received in revised form
21 June 2015
Accepted 22 June 2015
Available online 29 June 2015

Keywords:
Pyrimidine
Primaquine
Hybrid drugs
Antiplasmodial agents
Liver stage activity
Blood stage activity

ABSTRACT

A series of novel pyrimidine–primaquine hybrids were synthesized and their effectiveness against the blood and liver stages of malaria parasites was evaluated. The hybrids displayed enhanced liver stage *in vitro* activity against *P. berghei* liver stage infection.

1. Introduction

The magnitude of the devastation caused by malaria disease is significant, since as many as 250 million clinical cases (approx. 40 percent of human population) and a mortality of 584,000 people are reported annually [1].

Plasmodium falciparum is responsible for most malaria-associated mortality worldwide, and it is by far the predominant species in tropical and sub-tropical countries. Other species that cause malaria in humans are *Plasmoduim vivax, P. ovale, P. malariae* and *Plasmodium knowlesi. P. vivax* is less lethal than *P. falciparum* but, like *P. ovale*, can remain dormant in hepatic cells for many years and cause malaria recurrence/relapse. Similarly, *P. knowlesi* causes malaria in primates, but of late there are reports of malaria infections in humans also due to this species [2,3] The life cycle of malaria parasites [4] is initiated with the injection of *Plasmodium* sporozoites into their mammalian hosts during the bite of an infected female *Anopheles* mosquito. Once in circulation, sporozoites make their way to the liver, where they invade hepatocytes. During the exo-erythrocytic stage of their life cycle, sporozoites develop and multiply asymptomatically to produce tens of thousands of merozoites. Merozoites are eventually released into the blood stream, where they cyclically invade, multiply and rupture red blood cells, causing the symptoms of malaria. During this erythrocytic stage of their life cycle, some parasites develop into sexual forms called gametocytes that can be taken up by a mosquito upon a subsequent blood meal. The sexual phase of *Plasmodium* reproduction takes place in the mosquito's midgut and culminates in the production of thousands of sporozoites, which migrate to the mosquito's salivary glands, completing the cycle. In the armamentarium of antimalarial drugs, a major thrust is in the development of drugs that are efficacious against asexual blood (erythrocytic) stages of *P. falciparum*, which are responsible for illness but represent only a small proportion of the complex life-cycle of the parasite. In fact, the first obligatory phase of infection of a mammalian host occurs in the liver, where the parasite

* Corresponding author.
E-mail address: kamaljit.chem@gndu.ac.in (K. Singh).

http://dx.doi.org/10.1016/j.ejmech.2015.06.045
0223-5234/

asymptomatically infects and develops inside hepatocytes [4]. Despite constituting a privileged target for prophylactic intervention, the liver stage of infection is largely understudied and effective drugs against *Plasmodium* liver stages are very scarce [5]. This is particularly relevant in the case of infections by *P. vivax* and *P. ovale*, as these parasite species can form hypnozoites that remain dormant in liver cells for extended periods may lead to malaria relapses malaria.

The treatment regimen for malaria infection is complicated by the emergence of drug resistant parasite strains and resistance to the classical 4-aminoquinoline based chloroquine (CQ) **1**, a one-time effective blood stage schizonticidal drug [6,7]. The only highly effective and fast acting treatment effective against all species capable of causing human malaria resistant to other agents is represented by artemisinin (ART) and its derivatives that act on the asexual blood stages of malaria parasites [8]. They are generally implicated in the treatment of uncomplicated *P. falciparum* malaria as components of ART-based combination therapies (ACTs) in which the fast-acting ART is combined with another antimalarial agent with a long terminal half-life [9,10].

On the other hand, the 8-aminoquinoline based primaquine (PQ, Chart 1) **2** is the only drug that is used as a prophylactic agent against the clinically silent liver stage schizonts, and can eliminate hypnozoites, thus avoiding relapse of *P. vivax* infections [11]. PQ also acts against gametocytes produced during the life cycle sexual stages of the parasite and this activity disrupts the transmission of infection to mosquitoes [11]. Thus, PQ is frequently administered in combination with a blood-stage schizonticidal drug to achieve a radical cure of infections with *P. vivax or P. ovale* and to prevent relapses due to the development of subsequent blood-stage infections from hypnozoites [12,13]. However, unfortunately, the reliability of PQ has been questioned due to its possible side effects, which include methemoglobinemia and hemolytic anemia in glucose-6-phosphate dehydrogenase-deficient patients [14]. Besides, there are indications of the emergence of resistance to PQ [15].

Thus, in the struggle to fight malaria, new strategies are needed that provide cure for all *Plasmodium* species that infect human red blood cells, as well as replicative and dormant liver forms.

Hybrid drugs are purported to be the drugs of the future [16,17]. While a vast number of hybrids of chloroquine have been synthesized and evaluated [18–22], there are very few instances of evaluation of hybrids of PQ [23–26], for example, the ability of the primaquine-chloroquine hybrid **3** to inhibit (*in vitro* and *in vivo*) the liver and blood stages of mammalian Plasmodium infection has been demonstrated. Similarly, hybrids comprising of PQ and ART are able to inhibit both blood as well as liver stages of the parasite life cycle [23].

The enzyme dihydrofolate reductase (DHFR) has received considerable attention as a putative target of pyrimethamine **4** and other antifolate prophylaxis agents against *P. falciparum* infection. DHFR is implicated in the reduction of dihydrofolate to tetrahydrofolate (Fig. 1), which upon methylation results in the formation of N^5,N^{10}-methylene tetrahydrofolate coenzyme. The latter acts as a single carbon unit transfer agent to convert deoxyuridine monophosphate (dUMP) to deoxythymidine monophosphate (dTMP) in the presence of thymidylate synthase (TS) and is indirectly implicated in the metabolism of amino acids and purine nucleotides [27]. Overall, inhibition of DHFR prevents biosynthesis of DNA leading to death of the parasite. We have previously reported various types of hybrids containing pyrimidines and chloroquine pharmacophores, linked covalently through a variety of basic chains [28]. We have also evaluated the binding interactions and stoichiometry of binding with heme and μ-oxo heme. In addition these mechanistic studies have also revealed that these hybrids showed tendency to bind with AT rich pUC18 DNA and GC rich CT DNA.

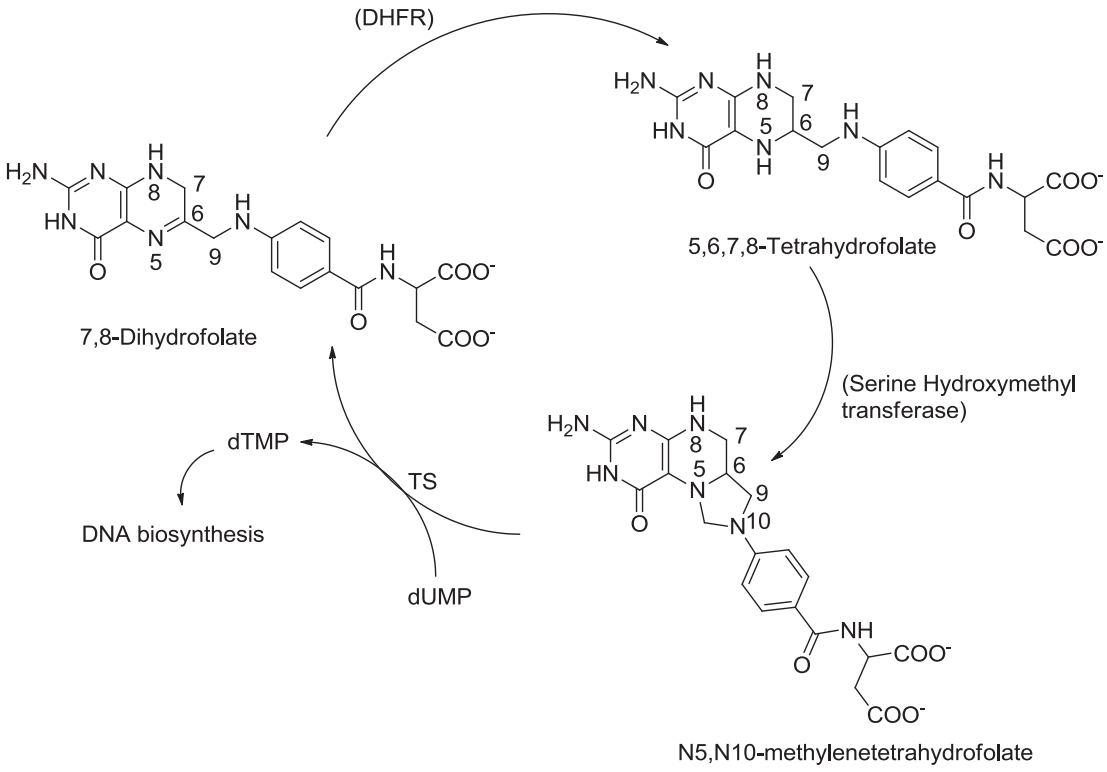

Fig. 1. Mode of action of dihydrofolate reductase (DHFR) in the biotransformation of dUMP to dTMP.

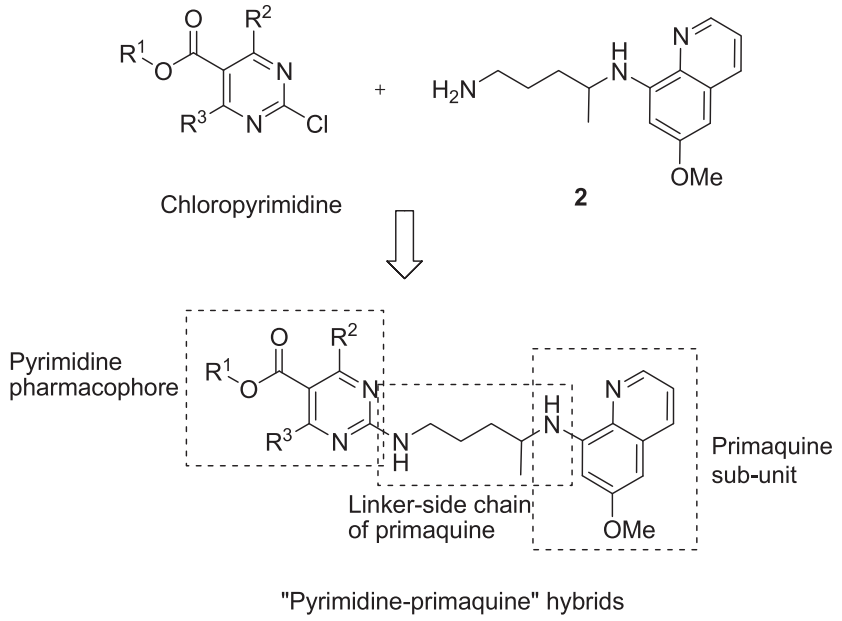

Fig. 2. Design strategy of "pyrimidine-primaquine" hybrids.

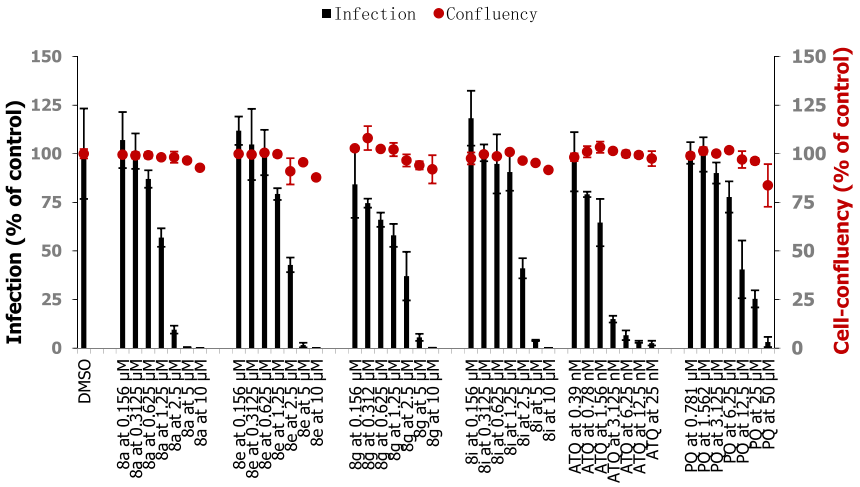

Fig. 3. Final screening of selected hybrid against liver stages. Activity (Infection scale, bars) and toxicity to hepatoma cells (cell confluency scale, circles).

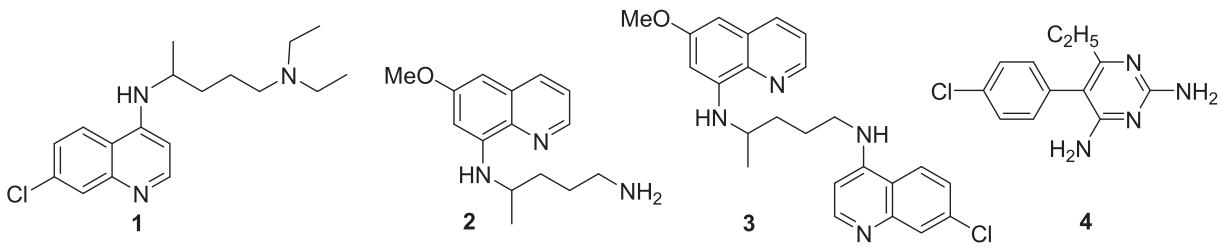

Chart 1. Antiplasmodial agents (chloroquine **1**, primaquine **2**, primaquine-chloroquine hybrid **3**, pyrimethamine **4**).

We hypothesized that pyrimidines, when combined with primaquine, will result in hybrids, which might display superior antimalarial activity. In this work, we exploit a dual-stage hybrid approach, wherein a pyrimidine pharmacophore has been covalently linked with PQ to obtain "pyrimidine-primaquine" hybrids (Fig. 2) for the first time. The choice of substituents on the hybrids was guided by our earlier investigations [28] wherein such substituents when incorporated on hybrids exert significant antimalarial action as well as impart adequate solubility.

2. Chemistry

The synthesis of target PQ-pyrimidine hybrids **8** is outlined in Scheme 1. The precursor 3,4-dihydropyrimidin-2(*1H*)-one **5** was

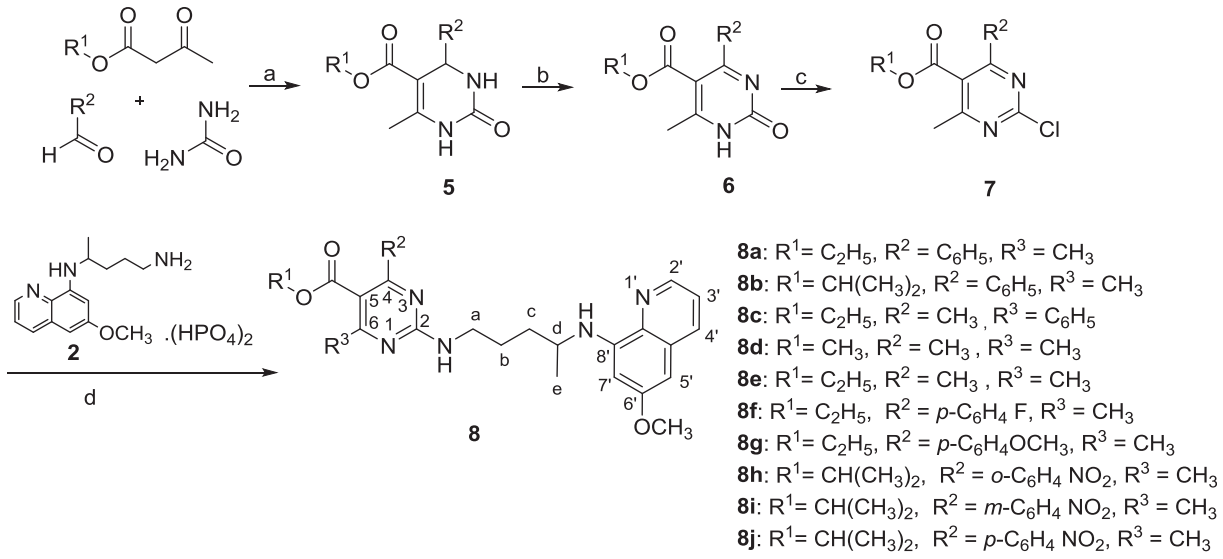

Scheme 1. (a) EtOH, HCl, rt; (b) 60% nitric acid, 0 °C; (c) $POCl_3$, 105 °C, 45 min; (d) NEt_3, DMF, rt. Atoms in **8** are numbered to facilitate assignment of ^{13}C NMR signals (Table 2).

prepared through NH_4Cl [29]/polyphosphate ester (PPE) [30]/HCl [31] catalyzed three-component Biginelli condensation of an alkyl/aryl acetoacetate, urea and appropriate aldehyde in C_2H_5OH/THF. Subsequent oxidation of **5** using 60% nitric acid [32] readily furnished pyrimidin-2(1*H*)-ones **6**, which upon chlorination with $POCl_3$ yielded 2-chloropyrimidin-2(1*H*)-ones **7**. The condensation of **7** with the commercially available primaquine biphosphate **2** in the presence of triethylamine in anhydrous DMF under an atmosphere of nitrogen at room temperature provided the target hybrids **8a**–**j** in excellent yields (Table 1). Structures of all the hybrids and intermediates were unambiguously established on the basis of spectral (^1H NMR, ^{13}C NMR, HRMS, FT IR) as well as microanalytical analysis.

3. Results and discussion

All the synthesized hybrids were tested against liver stages of the rodent parasite *P. berghei* and *in vitro* against blood stages of the CQ-sensitive *P. falciparum* NF54 strain (Table 1) in both assays. Atovaquone (ATQ) was used a positive control in liver stage testing whereas CQ and artesunate (ASN) were additional controls in the blood stage assays.

The hybrids **8a**–**j** displayed blood stage activity against *P. falciparum* with IC_{50} values in the range 1.93–6.46 μM. The analysis of the blood stage activity data of hybrids **8a**–**j** revealed that none of the hybrids exhibited better activity than the standard drugs (ASN, CQ and PQ), although the activity of hybrid **8j** was only 2.1 fold less than PQ. These results suggested that the conjugation of PQ with pyrimidine-5-carboxylate motif did not result in significant blood stage activity. The observed lack of blood stage activity of these hybrids may be attributed to the lack of aliphatic amine linkers in analogy to the work reported in the literature [24–26].

Furthermore, the nature of the substitution pattern on the pyrimidine pharmacophore has a significant effect on the *in vitro* antiplasmodial activity of hybrids **8**. The presence of a phenyl

Table 1
In vitro **a**ntiplasmodial activity, CC_{50} values and selectivity indices of hybrids **8a**–**j** and control drugs.

Hybrid	Yield (%)[a]	IC_{50} (μM)			SI
		Blood stage *Pf* NF54 strain[b,c]	Liver stage[d]	CC_{50} (μM)[e]	
8a	90	6.462	1.261 ± 0.310	>100	>79.3
8b	92	4.803	nd	–	–
8c	94	4.320	nd	–	–
8d	92	2.000	nd	–	–
8e	95	3.778	1.857 ± 0.302	61	32.6
8f	91	3.431	nd	–	–
8g	90	3.278	1.571 ± 0.248	>100	>63.6
8h	85	2.791	nd	–	–
8i	88	2.671	1.500 ± 0.594	>100	>66.6
8j	91	1.934	nd	–	–
PQ	–	0.892	8.428 ± 3.389	–	–
ATQ	–	nd	0.0018 ± 0.0003	–	–
CQ	–	0.0125	–		
ASN	–	0.0044	–		

nd = not determined.
[a] Isolated after column chromatography.
[b] Mean of three observation.
[c] Determined against CQ-sensitive strain.
[d] Determined against *P. berghei*.
[e] Toxicity determined against Huh 7 cell line.

substituent at C-4 of the pyrimidine core (**8a-b**) was detrimental to blood stage activity, whereas the presence of a *p*-nitrophenyl group at the C-4 position (**8j**) resulted in the most active hybrid of the series with an IC50 value of 1.93 μM. A comparison of the hybrids **8h**–**j** (*o*/*m*/*p*-nitro), **8f** (*p*-F), and **8g** (*p*-OCH_3) revealed that nitro substitution resulted in slightly improved blood stage activity. Switching the substituents (R^2 and R^3) in the isomeric hybrids **8a** and **8c** led to **8c** [IC_{50} = 4.320 μM], which was 1.5 fold more active against N54 strain of *P. falciparum* than **8a** (IC_{50} = 6.462 μM). The variation of the C-5 ester groups among the hybrids resulted in the *i*-propyl ester containing **8b** (IC_{50} = 4.803 μM) to be more active than **8a**.

Varying the substituents at C-6 position of the pyrimidine core suggested that **8e** bearing a methyl group at the C-6 position was marginally more active (**8e**: IC_{50} = 3.778 μM) than **8c** (IC_{50} = 4.320 μM) bearing a phenyl group at the same position. Thus, this brief SAR analysis suggested that the presence of phenyl substituents at C-4 or C-6 positions on the pyrimidine core led to lowering of blood stage antiplasmodial activity.

The potential of hybrids **8a**–**j** to inhibit the liver stages of *Plasmodium* infection was assessed on an infection system that uses a human heptoma cell line (Huh 7) and the rodent parasite *P. berghei*. In an initial screening we determined the effect of all the hybrids at 1 μM, 5 μM and 10 μM on infection and cell confluence. None of the hybrid **8a**–**j** significantly affected Huh7 cell proliferation (Table 1) indicating that the hybrids are non-toxic antimalarial agents. Moreover, these hybrids depicted high selectivity index (Table 1). An inspection of the data suggested that hybrids **8a**, **8e**, **8g** and **8i** led to the strongest decrease infection at the lowest tested concentration of 1 μM. Thus, we selected these hybrids for a dose response study and determined their IC_{50} values for the inhibition of hepatic *P. berghei* infection (Fig. 3). The comparison of IC_{50} values of hybrid **8** and standard drugs presented in Table 1 showed that the hybrids **8a**–**j** displayed superior activity relative to PQ but lower than ATQ. Among all the hybrids tested, hybrid **8a** (IC_{50} = 1.261 μM) showed the highest activity against the liver stage of infection, which is 6.7 fold greater than PQ (IC_{50} = 8.428 μM) albeit its blood stage activity is weaker. On the other hand, hybrid **8i** has good blood stage activity (IC_{50} = 2.671 μM), although lower than that of PQ (IC_{50} = 0.890 μM), along with excellent liver stage activity (IC_{50} = 1.5 μM) and is non-toxic (CC_{50} = > 100). Our preliminary liver stage activity studies revealed no *in vivo* activity for **8i**. However, **8i** may serve as good starting point for further structural optimization. Overall, it is concluded that the hybridization of PQ with pyrimidine-5-carboxylate enhances the inherent liver stage activity of the PQ motif.

4. Conclusions

The synthesis and antiplasmodial activity of novel class of hybrids combining pyrimidine-5-carboxylate motif with primaquine has been described. The synthesized hybrids exhibit enhanced liver stage activities in comparison to primaquine. One of the hybrids, **8i**, has good blood stage activity as well as excellent liver stage activity and may serve as good starting point for the development of potential antiplasmodial agents targeting both blood and liver stage infections.

5. Experimental

5.1. General

All liquid reagents were dried/purified following recommended drying agents and/or distilled over 4 Å molecular sieves. ^{1}H NMR (400 MHz) and ^{13}C (125 MHz) NMR spectra were recorded in $CDCl_3$ on a Bruker Avance II 400 spectrometer with chemical shifts being reported in parts per million (δ) relative to internal tetramethylsilane (TMS, δ 0.0, ^{1}H NMR) or chloroform ($CDCl_3$, δ77.0, ^{13}C NMR). Mass spectra were recorded at Department of Chemistry, Guru Nanak Dev University, Amritsar on a Bruker LC-MS MICROTOF II spectrometer. Elemental analysis was performed on FLASH EA 112 (Thermo electron Corporation) analyzer at Department of Chemistry, Guru Nanak Dev University, Amritsar and the results are quoted in %. IR spectra were recorded on Perkin Elmer FTIR-C92035 Fourier transform spectrometer in the range 400–4000 cm^{-1} using KBr pellets. For monitoring the progress of a reaction and for comparison purpose, thin layer chromatography (TLC) was performed on pre-coated aluminum sheets of Merck ($60F_{254}$, 0.2 mm) using an appropriate solvent system. The chromatograms were visualized under UV light. For column chromatography silica gel (60–120 mesh) was employed and eluents were ethyl acetate/hexane mixtures.

5.2. General procedure for synthesis of ***8***

To the stirred solution of primaquine biphosphate **2** (0.87 mmol) and triethylamine (2.6 mmol) in dry DMF (10 ml) nitrogen atmosphere, a solution of appropriate 2-chloropyrimidine **7** (0.87 mmol) in dry DMF (5 ml) was added. The reaction mixture was strirred at room temerature for 48 h under nitrogen atmosphere. The reaction mixture was concenterated under vacuum and the residue was purified by column chromatography using hexane/ethyl acetate as eluent to obtain corresponding **8**, which was then recrystallized from DCM/hexane to obtain yellow solid.

5.2.1. Ethyl 2-(4-(6-methoxyquinolin-8-ylamino)pentylamino)-6-methyl-4-phenylpyrimidin-5-carboxylate (***8a***)

Yellow solid. Yield: 90%. m.p: 65 °C. IR (KBr): ν_{max} 1266, 1565, 1710, 2928, 3058, 3385 cm^{-1}. ^{1}H NMR (400 MHz, $CDCl_3$, 25 °C): δ 0.91 (d, *J* = 6.2 Hz, 3H, $CHCH_3$), 1.29 (t, *J* = 6.6 Hz, 3H, ester-CH_3), 1.57–1.68 (m, 4H, 2 × CH_2), 2.44 (s, 3H, C6–CH_3), 3.48–3.50 (m, 2H, CH_2), 3.64–3.67 (m, 1H, $CHCH_3$), 3.85 (s, 3H, OCH_3), 4.01 (q, *J* = 6.6 Hz, 2H, ester-CH_2), 5.32 (br, 1H, NH), 5.99 (br, 1H, NH), 6.23–6.28 (m, 2H, ArH), 7.20–7.37 (m, 4H, ArH), 7.49 (s, 2H, ArH), 7.87 (d, *J* = 8.7 Hz, 1H, ArH), 8.50 (s, 1H, ArH). ^{13}C NMR (125 MHz, $CDCl_3$, 25 °C): δ 13.4, 20.5, 20.9, 26.3, 33.9, 41.1, 47.7, 55.1, 60.9, 96.7, 121.7, 127.9, 128.1, 129.3, 134.7, 139.2, 144.2, 159.4, 170.3. Anal. Calcd. For $C_{29}H_{33}N_5O_3$: C, 69.72; H, 6.66; N, 14.02; Found: C, 69.81; H, 6.73; N, 14.09. HRMS: *m/z* 500.2592 [M^+ + 1].

5.2.2. Isopropyl 2-(4-(6-methoxyquinolin-8-ylamino) pentylamino)-6-methyl-4-phenylpyrimidin-5-carboxylate (***8b***)

Yellow solid. Yield: 92%. m.p: 72 °C. IR (KBr): ν_{max} 1266, 1561, 1710, 2924, 3058, 3388 cm^{-1}. ^{1}H NMR (400 MHz, $CDCl_3$, 25 °C): δ 0.99 (d, *J* = 6.2 Hz, 6H, 2 × ester-CH_3), 1.31 (d, *J* = 6.4 Hz, 3H, CH_3), 1.70–1.81 (m, 4H, 2 × CH_2), 2.45 (s, 3H, C6–CH_3), 3.48–3.55 (m, 2H, CH_2), 3.66–3.68 (m, 1H, CH), 3.88 (s, 3H, OCH_3), 4.92–4.96 (m, 1H, ester-CH), 5.43 (br, 1H, NH), 6.02 (br, 1H, NH), 6.29 (d, *J* = 2.4 Hz, 1H, ArH), 6.33 (d, *J* = 2.4 Hz, 1H, ArH), 7.30 (dd, *J* = 4.2, 8.2 Hz, 1H, ArH), 7.36–7.41 (m, 3H, ArH), 7.53 (s, 2H, ArH), 7.92 (dd, *J* = 1.6, 8.2 Hz, 1H, ArH), 8.52 (dd, *J* = 1.6, 4.3 Hz, 1H, ArH). ^{13}C NMR (125 MHz, $CDCl_3$, 25 °C): δ 20.6, 21.3, 26.4, 34.0, 41.3, 47.8, 55.2, 68.7, 91.6, 96.7, 115.7, 121.8, 128.0, 128.2, 129.3, 129.9, 134.8, 135.3, 139.1, 144.2, 145.0, 159.4, 161.1, 168.3. Anal. Calcd. For $C_{30}H_{35}N_5O_3$: C, 70.15; H, 6.87; N, 13.63; Found: C, 69.99; H, 6.92; N, 13.56′. HRMS: *m/z* 514.2728 [M^+ + 1].

5.2.3. Ethyl 2-(4-(6-methoxyquinolin-8-ylamino)pentylamino)-4-methyl-6-phenylpyrimidin-5-carboxylate (***8c***)

Yellow solid. Yield: 94%. m.p: 68 °C. IR (KBr): ν_{max} 1266, 1560, 1712, 2926, 3057, 3388 cm^{-1}. ^{1}H NMR (400 MHz, $CDCl_3$, 25 °C):

δ 0.87 (t, J = 7.2 Hz, 3H, ester-CH_3), 1.21 (d, J = 6.3 Hz, 3H, CH_3), 1.63–1.75 (m, 4H, 2 × CH_2), 2.40 (s, 3H, C4–CH_3), 3.42–3.49 (m, 2H, CH_2), 3.59–3.61 (m, 1H, CH), 3.80 (s, 3H, OCH_3), 3.97 (q, J = 7.1 Hz, 2H, ester-CH_2), 5.42 (br, 1H, NH), 6.00 (br, 1H, NH), 6.22 (d, J = 2.4 Hz, 1H, ArH), 6.26 (d, J = 2.4 Hz, 1H, ArH), 7.23 (dd, J = 4.2, 8.2 Hz, 1H, ArH), 7.29–7.34 (m, 3H, ArH), 7.45–7.50 (m, 2H, ArH), 7.85 (dd, J = 1.6, 2.8 Hz, 1H, ArH), 8.45 (dd, J = 1.6, 4.2 Hz, 1H, ArH). ^{13}C NMR (125 MHz, $CDCl_3$, 25 °C): δ 13.5, 20.6, 26.3, 34.0, 41.3, 47.8, 55.2, 61.0, 91.6, 96.8, 115.1, 121.8, 127.9, 128.2, 129.4, 129.9, 134.9, 135.2, 139.1, 144.2, 144.9, 159.4, 166.2, 168.8. Anal. Calcd. For $C_{29}H_{33}N_5O_3$: C, 69.72; H, 6.66; N, 14.02; Found: C, 69.65; H, 6.78; N, 13.94. HRMS: m/z 500.2583 [M^+ + 1].

5.2.4. Methyl 2-(4-(6-methoxyquinolin-8-ylamino)pentylamino)-4,6-dimethylpyrimidin-5-carboxylate (**8d**)

Yellow solid. Yield: 92%. m.p: 44 °C. IR (KBr): ν_{max} 1266, 1566, 1711, 2928, 3083, 3388 cm^{-1}. ^{1}H NMR (400 MHz, $CDCl_3$, 25 °C): δ 1.28 (d, J = 6.0 Hz, 3H, CH_3), 1.74–1.72 (m, 4H, 2 × CH_2), 2.38 (s, 6H, C4 & C6–CH_3), 3.44–3.49 (m, 2H, CH_2), 3.64–3.67 (m, 1H, CH), 3.83–3.89 (m, 6H, OCH_3 & ester CH_3), 5.32 (br, 1H, NH), 6.00 (br, 1H, NH), 6.26 (s, 1H, ArH), 6.31 (d, J = 2.1 Hz, 1H, ArH), 7.24–7.29 (m, 1H, ArH), 7.89 (d, J = 8.1 Hz, 1H, ArH), 8.50 (d, J = 4.2 Hz, 1H, ArH). ^{13}C NMR (125 MHz, $CDCl_3$, 25 °C): δ 20.8, 23.3, 25.5, 34.7, 42.4, 47.3, 55.9, 63.5, 96.2, 99.3, 119.9, 121.7, 124.4, 132.1, 135.7, 145.3, 147.1, 160.5, 168.2. Anal. Calcd. For $C_{23}H_{29}N_5O_3$: C, 65.23; H, 6.90; N, 16.54; Found: C, 65.31; H, 6.94; N, 16.46. HRMS: m/z 424.2335 [M^+ + 1].

5.2.5. Ethyl 2-(4-(6-methoxyquinolin-8-ylamino)pentylamino)-4,6-dimethylpyrimidin-5-carboxylate (**8e**)

Yellow solid. Yield: 95%. m.p: 47 °C. IR (KBr): ν_{max} 1266, 1520, 1561, 1710, 2924, 3058, 3388 cm^{-1}. ^{1}H NMR (400 MHz, $CDCl_3$, 25 °C): δ 0.78 (d, J = 5.7 Hz, 3H, CH_3), 1.29 (t, J = 7.2 Hz, 3H, ester-CH_3), 1.66–1.70 (m, 4H, 2 × CH_2), 2.33 (s, 6H, C4 & C6–CH_3), 3.41 (t, J = 6.0 Hz, 2H, CH_2), 3.57–3.61 (m, 1H, CH), 3.81 (s, 3H, OCH_3), 4.26 (q, J = 7.2 Hz, 2H, ester-CH_2), 5.18 (br, 1H, NH), 5.95 (br, 1H, NH), 6.21 (s, 1H, ArH), 6.25 (d, J = 2.4 Hz, 1H, ArH), 7.23 (t, J = 4.2 Hz, 1H, ArH), 7.85 (d, J = 8.4 Hz, 1H, ArH), 8.45 (dd, J = 1.5 Hz, 4.2 Hz, 1H, ArH). ^{13}C NMR (125 MHz, $CDCl_3$, 25 °C): δ 14.1, 21.4, 22.5, 25.3, 34.9, 45.2, 46.9, 55.7, 60.9, 96.3, 99.7, 121.0, 125.4, 132.3, 134.8, 144.9, 146.1, 160.3, 166.4. Anal. Calcd. For $C_{24}H_{31}N_5O_3$: C, 65.88; H, 7.14; N, 16.01; Found: C, 65.80; H, 6.99; N, 16.11. HRMS: m/z 438.2498 [M^+ + 1].

5.2.6. Ethyl 4-(4-fluorophenyl)-2-(4-(6-methoxyquinolin-8-ylamino)pentylamino)-6-methylpyrimidin-5-carboxylate (**8f**)

Yellow solid. Yield: 91%. m.p: 60 °C. IR (KBr): ν_{max} 1266, 1564, 1710, 2920, 3084, 3388 cm^{-1}. ^{1}H NMR (400 MHz, $CDCl_3$, 25 °C): δ 1.01 (t, J = 6.9 Hz, 3H, ester-CH_3), 1.31 (d, J = 6.3 Hz, 3H, CH_3), 1.77–1.81 (m, 4H, 2 × CH_2), 2.47 (s, 3H, C6–CH_3), 3.52–3.55 (m, 2H, CH_2), 3.65–3.67 (m, 1H, CH), 3.88 (s, 3H, OCH_3), 4.04 (q, J = 7.2 Hz, 2H, CH_2), 5.30 (br, 1H, NH), 6.10 (br, 1H, NH), 6.31 (s, 1H, ArH), 6.35 (d, J = 2.4 Hz, 1H, ArH), 7.07 (t, J = 7.1 Hz, 2H, ArH), 7.29–7.40 (m, 1H, ArH), 7.53 (m, 1H, ArH), 7.95 (m, 2H, ArH), 8.52 (dd, J = 1.5, 3.9 Hz, 1H, ArH). ^{13}C NMR (125 MHz, $CDCl_3$, 25 °C): δ 13.7, 20.7, 21.2, 26.5, 34.2, 41.3, 48.0, 55.4, 61.1, 96.9, 122.0, 128.1, 128.4, 129.5, 130.1, 134.9, 139.4, 144.5, 159.6, 170.6. Anal. Calcd. For $C_{29}H_{32}FN_5O_3$: C, 67.29; H, 6.23; N, 13.53; Found: C, 67.21; H, 6.37; N, 13.61. HRMS: m/z 518.2582 [M^+ + 1].

5.2.7. Ethyl 2-(4-(6-methoxyquinolin-8-ylamino)pentylamino)-6-methyl-4-(4-methoxyphenyl)pyrimidin-5-carboxylate (**8g**)

Yellow solid. Yield: 90%. m.p: 45 °C IR (KBr): ν_{max} 1268, 1524, 1566, 1710, 2929, 3081, 3387 cm^{-1}. ^{1}H NMR (400 MHz, $CDCl_3$, 25 °C): δ 1.06 (t, J = 7.1 Hz, 3H, ester-CH_3), 1.29 (d, J = 6.3 Hz, 3H, CH_3), 1.70–1.81 (m, 4H, 2 × CH_2), 2.44 (s, 3H, C6–CH_3), 3.48–3.55 (m, 2H, CH_2), 3.65–3.66 (m, 1H, CH), 3.83 (s, 3H, OCH_3), 3.88 (s, 3H, OCH_3), 4.10 (q, J = 7.1 Hz, 2H, CH_2), 5.37 (br, 1H, NH), 6.04 (br, 1H, NH), 6.29 (d, J = 2.4 Hz, 1H, ArH), 6.33 (d, J = 2.4 Hz, 1H, ArH), 6.88–6.92 (m, 2H, ArH), 7.28 (dd, J = 4.2, 8.2 Hz, 1H, ArH), 7.53 (d, J = 8.0 Hz, 2H, ArH), 7.90 (dd, J = 1.6, 8.2 Hz, 1H, ArH), 8.52 (dd, J = 1.5, 4.1 Hz, 1H, ArH). ^{13}C NMR (125 MHz, $CDCl_3$, 25 °C): δ 13.7, 20.6, 22.8, 26.4, 34.0, 41.3, 47.8, 55.2, 55.3, 61.0, 91.6, 96.7, 113.6, 114.8, 121.8, 129.6, 129.9, 131.4, 134.7, 135.3, 144.3, 145.0, 159.4, 160.8, 161.1, 165.1, 169.3. Anal. Calcd. For $C_{30}H_{35}N_5O_4$: C, 68.03; H, 6.66; N, 13.22; Found: C, 67.89; H, 6.74; N, 13.05. HRMS: m/z 530.2678 [M^+ + 1].

5.2.8. Isopropyl 2-(4-(6-methoxyquinolin-8-ylamino)pentylamino)-6-methyl-4-(2-nitrophenyl)pyrimidin-5-carboxylate (**8h**)

Yellow solid. Yield: 85%. m.p: 84 °C. IR (KBr): ν_{max} 1266, 1385, 1524, 1566, 1712, 2929, 3082, 3388 cm^{-1}. ^{1}H NMR (400 MHz, $CDCl_3$, 25 °C): δ 0.90 (d, J = 6.4 Hz, 6H, 2 × ester-CH_3), 1.30 (d, J = 5.3 Hz, 3H, CH_3), 1.67–1.74 (m, 4H, 2 × CH_2), 2.58 (s, 3H, C6–CH_3), 3.36–3.56 (m, 2H, CH_2), 3.58–3.65 (m, 1H, CH), 3.88 (s, 3H, OCH_3), 4.84–4.86 (m, 1H, ester-CH), 6.00 (br, 1H, NH), 6.28 (s, 1H, ArH), 6.33 (d, J = 2.3 Hz, 1H, ArH), 7.27–7.32 (m, 1H, ArH), 7.44 (br, 1H, NH), 7.52–7.62 (m, 2H, ArH), 7.93 (d, J = 7.4 Hz, 1H, ArH), 8.04 (t, J = 7.0 Hz, 1H, ArH), 8.14 (d, J = 7.7 Hz, 1H, ArH), 8.52 (dd, J = 1.6, 4.2 Hz, 1H, ArH). ^{13}C NMR (125 MHz, $CDCl_3$, 25 °C): δ 20.6, 21.2, 26.2, 33.9, 41.5, 47.8, 55.2, 62.1, 91.6, 95.8, 119.3, 121.8, 124.3, 129.0, 148.1, 154.0, 161.0, 166.3, 179.7, 184.3, 189.4, 190.9. Anal. Calcd. For $C_{30}H_{34}N_6O_5$: C, 64.50; H, 6.13; N, 15.04; Found: C, 64.59; H, 6.26; N, 15.09. HRMS: m/z 559.2583 [M^+ + 1].

5.2.9. Isopropyl 2-(4-(6-methoxyquinolin-8-ylamino)pentylamino)-6-methyl-4-(3-nitrophenyl)pyrimidin-5-carboxylate (**8i**)

Yellow solid. Yield: 88%. m.p: 67 °C. IR (KBr): ν_{max} 1266, 1385, 1524, 1566, 1712, 2929, 3082, 3388 cm^{-1}. ^{1}H NMR (400 MHz, $CDCl_3$, 25 °C): δ 1.08 (d, J = 6.1 Hz, 6H, 2 × ester-CH_3), 1.30 (d, J = 6.2 Hz, 3H, CH_3), 1.66–1.79 (m, 4H, 2 × CH_2), 2.49 (s, 3H, C6–CH_3), 3.49–3.53 (m, 2H, CH_2), 3.65–3.66 (m, 1H, CH), 3.88 (s, 3H, OCH_3), 5.01–5.20 (m, 1H, ester-CH), 5.45 (br, 1H, NH), 6.10 (br, 1H, NH), 6.28 (d, J = 2.4 Hz, 1H, ArH), 6.33 (d, J = 2.4 Hz, 1H, ArH), 7.29–7.32 (m, 1H, ArH), 7.56 (t, J = 7.8 Hz, 1H, ArH), 7.80–7.91 (m, 2H, ArH), 8.28 (d, J = 7.3 Hz, 1H, ArH), 8.41 (s, 1H, ArH), 8.52 (s, 1H, ArH). ^{13}C NMR (125 MHz, $CDCl_3$, 25 °C): δ 20.6, 21.4, 23.3, 26.3, 34.0, 41.3, 47.8, 55.2, 69.1, 91.7, 96.8, 121.8, 123.3, 123.9, 129.2, 129.9, 134.1, 134.8, 140.8, 148.2, 159.5, 161.1, 167.1. Anal. Calcd. For $C_{30}H_{34}N_6O_5$: C, 64.50; H, 6.13; N, 15.04; Found: C, 64.62; H, 6.28; N, 15.17. HRMS: m/z 559.2599 [M^+ + 1].

5.2.10. Isopropyl 2-(4-(6-methoxyquinolin-8-ylamino)pentylamino)-6-methyl-4-(4-nitrophenyl)pyrimidin-5-carboxylate (**8j**)

Yellow solid. Yield: 91%. m.p: 90 °C. IR (KBr): ν_{max} 1266, 1385, 1524, 1566, 1712, 2929, 3082, 3388 cm^{-1}. ^{1}H NMR (400 MHz, $CDCl_3$, 25 °C): δ 1.03 (d, J = 6.2 Hz, 6H, 2 × ester-CH_3), 1.27 (d, J = 6.2 Hz, 3H, CH_3), 1.69–1.81 (m, 4H, 2 × CH_2), 2.48 (s, 3H, C6–CH_3), 3.50–3.52 (m, 2H, CH_2), 3.65–3.67 (m, 1H, CH), 3.88 (s, 3H, OCH_3), 4.95–4.97 (m, 1H, ester-CH), 5.48 (br, 1H, NH), 6.02 (br, 1H, NH), 6.28 (s, 1H, ArH), 6.34 (d, J = 2.4 Hz, 1H, ArH), 7.30 (dd, J = 4.2, 8.2 Hz, 1H, ArH), 7.66 (d, J = 8.6 Hz, 2H, ArH), 7.92 (dd, J = 1.4, 8.2 Hz, 1H, ArH), 8.22 (d, J = 7.7 Hz, 2H, ArH), 8.52 (dd, J = 1.5, 4.2 Hz, 1H, ArH). ^{13}C NMR (125 MHz, $CDCl_3$, 25 °C): δ 20.6, 21.0, 22.7, 26.3, 33.9, 41.3, 47.7, 55.2, 69.0, 91.6, 96.8, 115.4, 121.8, 123.4, 129.1, 129.9, 134.8, 135.3, 144.3, 144.9, 145.5, 148.1, 159.4, 161.1, 163.9, 167.4. Anal. Calcd. For $C_{30}H_{34}N_6O_5$: C, 64.50; H, 6.13; N, 15.04; Found: C, 64.44; H, 6.07; N, 15.20. HRMS: m/z 559.2593 [M^+ + 1].

Table 2
Assignment (partial) of signals in ^{13}C NMR spectra of **8a**–**j**.

Compound	Partial ^{13}C NMR assignment (δ/ppm)											
	C-6 Me	C-5 ester	5	6	a	b	c	d	e	C-6′ OMe	C-4 methyl or substituent on C-4 aromatic ring	CO
8a	20.9	13.4, 60.9	96.7	159.4	41.1	26.3	33.9	47.7	20.5	55.1	–	170.3
8b	21.3	21.3, 68.7	96.7	159.4	41.3	26.4	34.0	47.8	20.6	55.2	–	168.3
8c	20.6	13.5, 61.0	96.8	159.4	41.3	26.3	34.0	47.8	20.6	55.2	26.3	168.8
8d	23.3	63.5	96.2	160.5	42.4	25.5	34.7	47.3	20.8	55.9	20.8	168.2
8e	22.5	14.1, 60.9	96.3	160.3	45.2	25.3	34.9	46.9	21.4	55.7	21.4	166.4
8f	21.2	13.7, 61.3	96.9	159.6	41.3	26.5	34.2	48.0	20.7	55.4	–	170.6
8g	22.8	13.7, 61.0	96.7	159.4	41.3	26.4	34.0	47.8	20.6	55.2	55.3	169.3
8h	21.2	21.2, 62.1	95.8	161.0	41.5	26.2	33.9	47.8	20.6	55.2	148.1	166.3
8i	23.3	21.4, 69.1	96.8	159.5	41.3	26.3	34.0	47.8	20.6	55.2	148.2	167.1
8j	22.7	21.0, 69.0	96.8	159.4	41.3	26.3	33.9	47.7	20.6	55.2	148.1	167.4

Assignment of the key signals in the ^{13}C NMR spectra of **8a**–**j** is presented in Table 2.

6. *In vitro* blood stage activity assay

The test samples were tested in triplicate on one or two separate occasions against chloroquine sensitive (CQ^S) NF54 strain of *P. falciparum*. Continuous *in vitro* cultures of asexual erythrocyte stages of *P. falciparum* were maintained using a modified method of Trager and Jensen [33]. Quantitative assessment of antiplasmodial activity *in vitro* was determined *via* the parasite lactate dehydrogenase assay using a modified method described by Makler [34].

The test samples were prepared to a 20 mg/ml stock solution in 100% DMSO. Samples were tested as a suspension. Stock solutions were stored at −20 °C. Further dilutions were prepared on the day of the experiment. Chloroquine (CQ) and artesunate were used as the reference drugs in all experiments. A full dose–response was performed for all compounds to determine the concentration inhibiting 50% of parasite growth (IC_{50}–value). Test samples were tested at a starting concentration of 100 μg/ml, which was then serially diluted 2-fold in complete medium to give 10 concentrations; with the lowest concentration being 0.2 μg/ml. The same dilution technique was used for all samples. Reference drugs were tested at a starting concentration of 1000 ng/ml. Active samples were tested at a starting concentration of 1000 ng/ml. The highest concentration of solvent to which the parasites were exposed to had no measurable effect on the parasite viability (data not shown). The IC_{50}-values were obtained using a non-linear dose response curve fitting analysis *via* Graph Pad Prism v.4.0 software.

7. *In vitro* liver stage activity assay

Inhibition of liver-stage infection by test compounds was determined by measuring the luminescence intensity in Huh-7 cells infected with a firefly luciferase-expressing *P. berghei* line, as previously described [35]. Briefly, Huh-7 cells, a human hepatoma cell line, were cultured in 1640 RPMI medium supplemented with 10% *v/v* fetal bovine serum, 1% *v/v* nonessential amino acids, 1% *v/v* penicillin/streptomycin, 1% *v/v* glutamine, and 10 mM 4-(2-hydroxyethyl)-1-piperazineethanesulfonic acid (HEPES), pH 7, and maintained at 37 °C with 5% CO_2. For infection assays, Huh-7 cells (1.0×10^4 per well) were seeded in 96-well plates the day before drug treatment and infection. The medium was replaced by medium containing the appropriate concentration of each compound approximately 1 h prior to infection with sporozoites freshly obtained through disruption of salivary glands of infected female *Anopheles stephensi* mosquitoes. Sporozoite addition was followed by centrifugation at 1700 g for 5 min. Parasite infection load was measured 48 h after infection by a bioluminescence assay (Biotium). The effect of the compounds on the viability of Huh-7 cells was assessed by the Alamar Blue assay (Invitrogen, U.K.) using the manufacturer's protocol.

8. *In vivo* liver stage activity assay

C57Bl/6J mice were infected by intravenous inoculation of 5×10^3 luciferase-expressing *P. berghei* ANKA sporozoites freshly dissected from the salivary glands of infected *A. stephensi* mosquitoes. Compound **8i** was dissolved in DMSO (stock solution) and a 50 mg/kg bw suspension of the compound in sunflower oil was administered at by oral gavage injection 8 h prior to infection, at the time of infection, and 24 h after infection. An equivalent amount of drug vehicle was injected in control mice.

Determination of liver parasite loads *in vivo* was carried out as previously described [36]. Briefly, livers were collected and homogenized in a denaturing solution (4 M guanidine thiocyanate; 25 mM sodium citrate [pH 7], 0.5% sarcosyl, and 0.7% β-mercaptoethanol in diethyl pyrocarbonate-treated water) 47 h after sporozoite injection. Total RNA was extracted using the Qiagen RNeasy Mini kit according to the manufacturer's instructions. RNA for infection measurements was converted into cDNA by using the Nzytech kit according to the manufacturer's protocol. The quantitative real-time PCRs (qRT-PCRs) used the Applied Biosystems Power SYBR green PCR master mix and were performed according to the manufacturer's instructions on an ABI Prism 7500 Fast system (Applied Biosystems). Amplification reactions were carried out in a total reaction volume of 20 μl, using 1 μg cDNA and employing *P. berghei* ANKA 18S rRNA gene- or housekeeping gene-specific primers. Relative amounts of *P. berghei* ANKA mRNA were calculated against the amount of the hypoxanthine guanine phosphoribosyltransferase (HPRT) housekeeping gene. Primer sequences specific to each gene were as follows: for the *P. berghei* ANKA 18S rRNA gene, 5′-AAG CAT TAA ATA AAG CGA ATA CAT CCT TAC-3′ and 5′-GGA GAT TGG TTT TGA CGT TTA TGT G-3′; for the mouse HPRT gene, 5′-TGC TCG AGA TGT GAT GAA GG-3′ and 5′-TCC CCT GTT GAC TGG TCA TT-3′; and for the human HPRT gene, 5′-TGC TCG AGA TGT GAT GAA GG-3′ and 5′-TCC CCT GTT GAC TGG TCA TT-3′.

Acknowledgments

We gratefully acknowledge financial assistance from CSIR, New Delhi and Fundação para a Ciência e Tecnologia, Portugal (grant PTDC/SAU-MIC/117060/2010 to MP). H.K. thanks CSIR, New Delhi for senior research fellowship (F. No. 09/254 (0195)/2009-EMR-I). The University of Cape Town, South African Medical Research Council, and South African Research Chairs Initiative of the Department of Science and Technology, administered through the

South African National Research Foundation are gratefully acknowledged for support (K.C).

Appendix A. Supplementary data

Supplementary data related to this article can be found at http://dx.doi.org/10.1016/j.ejmech.2015.06.045.

References

[1] World Malaria Report, World Health Organization, Geneva, 2012. Available from, http://www.who.int/iris/bitstream/10665/78945/1/9789241564533_eng.pdf.
[2] C. Daneshvar, Clinical and laboratory features of human *Plasmodium knowlesi* infection, Clin. Infect. Dis. 49 (2009) 852–860.
[3] M.D.S. Sabbatani, M.D. Sirio Fiorino, M.D. Roberto Manfredi, The emerging of the fifth malaria parasite*(Plasmodium knowlesi)*. A public health concern? Braz. J. Infect. Dis. 14 (2010) 1–13.
[4] M. Prudêncio, A. Rodriguez, M.M. Mota, The silent path to thousands of merozoites: the *Plasmodium* liver stage, Nat. Rev. Microbiol. 4 (2006) 849–856.
[5] T. Rodrigues, M. Prudêncio, R. Moreira, M.M. Mota, F. Lopes, Targeting the liver stage of malaria parasites: a yet unmet goal, J. Med. Chem. 55 (2012) 995–1012.
[6] P. Winstanley, S. Ward, Malaria chemotherapy, Adv. Parasitol. 61 (2006) 47–76.
[7] T.J. Egan, Quinoline antimalarials, Expert Opin. Ther. Pat. 11 (2001) 185–209.
[8] World Health Organization, Guidelines for the Treatment of Malaria, second ed., WHO Press, Geneva, 2010.
[9] World Health Organization, Global Report on Antimalarial Drug Efficacy and Drug Resistance: 2000–2010, WHO Press, Geneva, 2010.
[10] R.N. Price, Artemisinin drugs: novel antimalarial agents, Exp. Opin. Invest. Drugs 9 (2000) 1815–1827.
[11] L. Tilley, P. Loria, M. Foley, Chloroquine and other quinoline antimalarials, in: P.J. Rosenthal (Ed.), Antimalarial Chemotherapy: Mechanisms of Action, Resistance, and New Directions in Drug Discovery, Humana Press, Totowa, NJ, 2001.
[12] Pasaribu, W. Chokejindachai, C. Sirivichayakul, N. Tanomsing, I. Chavez, E. Tjitra, S. Pasaribu, M. Imwong, N. White, J.A.M. Dondorp, A randomized comparison of dihydroartemisinin-piperaquine and artesunate-amodiaquine combined with primaquine for radical treatment of vivax malaria in Sumatera, Indonesia, J. Infect. Dis. 208 (2013) 1906–1913.
[13] S. Pukrittayakamee, J. Tarning, P. Jittamala, P. Charunwatthana, S. Lawpoolsri, S.J. Lee, W. Hanpithakpong, B. Hanboonkunupakarn, N.P.J. Day, E.A. Ashley, N.J. White, Pharmacokinetic interactions between primaquine and chloroquine, Antimicrob. Agents Chemother. 58 (2014) 3354–3359.
[14] G.D. Shanks, A.J. Oloo, G.M. Aleman, C. Ohrt, F.W. Klotz, D. Braitman, J. Horton, R. Brueckner, A new primaquine analogue, tafenoquine (WR 238605), for prophylaxis against *Plasmodium falciparum* malaria, Clin. Infect. Dis. 33 (2001) 1968–1974.
[15] W.E. Collins, G.M. Jeffery, Primaquine resistance in *Plasmoduim vivax*, Am. J. Trop. Med. Hyg. 55 (1996) 243–249.
[16] F.W. Muregi, A. Ishih, Next-generation antimalarial drugs: hybrid molecules as a new strategy in drug design, Drug Dev. Res. 71 (2010) 20–32.
[17] S.S. Chauhan, M. Sharma, P.M.S. Chauhan, Trioxaquines: hybrid molecules for the treatment of malaria, Drug News Perspect. 23 (2010) 632–646.
[18] F. Cosledan, L. Fraisse, A. Pellet, F. Guillou, B. Mordmüller, P.G. Kremsner, A. Moreno, D. Mazier, J.-P. Maffrand, B. Meunier, Selection of a trioxaquine as an antimalarial drug candidate, Proc. Natl. Acad. Sci. U. S. A. 105 (2008) 17579–17584.
[19] B.C. Perez, C. Teixeira, I.S. Albuquerque, J. Gut, P.J. Rosenthal, J.R.B. Gomes, M. Prudêncio, P. Gomes, N-Cinnamoylated chloroquine analogues as dual-stage antimalarial leads, J. Med. Chem. 56 (2013) 556–567.
[20] P.F. Salas, C. Herrmann, J.F. Cawthray, C. Nimphius, A. Kenkel, J. Chen, C. de Kock, P.J. Smith, B.O. Patrick, M.J. Adam, C. Orvig, Structural characteristics of chloroquine-bridged ferrocenophane analogues of ferroquine may obviate malaria drug resistance mechanisms, J. Med. Chem. 56 (2013) 1596–1613.
[21] Nisha, J. Gut, P.J. Rosenthal, V. Kumar, β-amino-alcohol tethered 4-aminoquinoline-isatin conjugates: synthesis and antimalarial evaluation, Eur. J. Med. Chem. 84 (2014) 566–573.
[22] A. Mishra, H. Batchu, K. Srivastava, P. Singh, P.K. Shukla, S. Batra, Synthesis and evaluation of new diaryl ether and quinoline hybrids as potential antiplasmodial and antimicrobial agents, Bioorg. Med. Chem. Lett. 24 (2014) 1719–1723.
[23] R. Capela, G.G. Cabal, P.J. Rosenthal, J. Gut, M.M. Mota, R. Moreira, F. Lopes, M. Prudencio, Design and evaluation of primaquine-artemisinin hybrids as a multistage antimalarial strategy", Antimicrob. Agents Chemother. 55 (2011) 4698–4706.
[24] D. Miranda, R. Capela, I.S. Albuquerque, P. Meireles, I. Paiva, F. Nogueira, R. Amewu, J. Gut, P.J. Rosenthal, R. Oliveira, M.M. Mota, R. Moreira, F. Marti, M. Prudencio, P.M. O"Neill, F. Lopes, Novel endoperoxide-based transmission-blocking antimalarials with liver- and blood-schizontocidal activities, ACS Med. Chem. Lett. 5 (2014) 108–112.
[25] J. Matos, N. Vale, M.S. Collins, J. Gut, P.J. Rosenthal, M.T. Cushion, R. Moreiraf, P. Gomes, PRIMACENES: novel non-cytotoxic primaquine-ferrocene conjugates with anti-*Pneumocystis carinii* activity, Med. Chem. Commun. 1 (2010) 199–201.
[26] B. Perez, C. Teixeira, I.S. Albuquerque, J. Gut, P.J. Rosenthal, M. Prudencio, P. Gomes, PRIMACINS, N-cinnamoyl-primaquine conjugates, with improved liver-stage antimalarial activity, Med. Chem. Commun. 3 (2012) 1170–1172.
[27] (a) C.E. Garrett, J.A. Coderre, T.D. Meek, E.P. Garvey, S.M. Beverly, D.V. Santi, A bifunctional thymidylate synthetase-dihydrofolate reductase in protozoa, Mol. Biochem. Parasitol. 11 (1984) 257–265;
(b) V.F. Roche, Mechanism based inhibitors of deoxythymidine monophosphate synthesis as antineoplastic agents, Am. J. Pharm. Educ. 58 (1994) 196–203.
[28] (a) K. Singh, H. Kaur, K. Chibale, J. Balzarini, S. Little, P.V. Bharatam, 2-Aminopyrimidine based 4-aminoquinoline anti-plasmodial agents. Synthesis, biological activity, structure-activity relationship and mode of action studies, Eur. J. Med. Chem. 52 (2012) 82–97;
(b) K. Singh, H. Kaur, K. Chibale, J. Balzarini, Synthesis of 4-aminoquinoline–pyrimidine hybrids as potent antimalarials and their mode of action studies, Eur. J. Med. Chem. 66 (2013) 314–323;
(c) K. Singh, H. Kaur, P. Smith, C. de Kock, K. Chibale, J. Balzarini, Quinoline–pyrimidine hybrids: synthesis, antiplasmodial activity, SAR and mode of action studies, J. Med. Chem. 57 (2014) 435–448.
[29] A. Shaabani, A. Bazgir, F. Teimouri, Ammonium chloride-catalyzed one-pot synthesis of 3,4-dihydropyrimidin-2-(1H)-ones under solvent-free conditions, Tetrahedron Lett. 44 (2003) 857–859.
[30] F.S. Falsone, C.O. Kappe, The Biginelli dihydropyrimidone synthesis, Arkivoc ii (2001) 122–134.
[31] P. Biginelli, Aldureids of ethylic acetoacetate and ethylic oxaloacetate, Gazz. Chim. Ital. 23 (1893) 360–413.
[32] A. Puchala, F. Belaj, J. Bergman, C.O. Kappe, On the reaction of 3,4- dihydropyrimidones with nitric acid. Preparation and X-ray structure analysis of a stable nitrolic acid, J. Heterocycl. Chem. 38 (2001) 1345–1352.
[33] W. Trager, J.B. Jensen, Human malaria parasite in continuous culture, Science 193 (1976) 673–675.
[34] M.T. Makler, J.M. Ries, J.A. Williams, J.E. Bancroft, R.C. Piper, B.L. Gibbins, D.J. Hinrichs, Parasite lactate dehydrogenase as an assay for *Plasmodium falciparum* drug sensitivity, Am. J. Trop. Med. Hyg. 48 (1993) 739–741.
[35] I.H. Ploemen, M. Prudêncio, B.G. Douradinha, J. Ramesar, J. Fonager, G.J. van Gemert, A.J. Luty, C.C. Hermsen, R.W. Sauerwein, F.G. Baptista, M.M. Mota, A.P. Waters, I. Que, C.W. Lowik, S.M. Khan, C.J. Janse, B.M. Franke-Fayard, Visualisation and quantitative analysis of the rodent malaria liver stage by real time imaging, PLoS ONE 4 (2009) e7881.
[36] M. Prudêncio, C.D. Rodrigues, M. Hannus, C. Martin, E. Real, L.A. Gonçalves, C. Carret, R. Dorkin, I. Röhl, K. Jahn-Hoffmann, A.J.F. Luty, R. Sauerwein, C. Echeverri, J.M.M. Motaet, Kinome-wide RNAi screen implicates at least 5 host hepatocyte kinases in *Plasmodium sporozoite* infection, PLoS Pathog. 4 (2008) e1000201.